Title

The impact of boundary conditions and fluid velocity on damping for a fluid conveying pipe in a viscous fluid

Authors

Kjolsing, Eric
Todd, Michael

Publication Date

2016-04-15

DOI

10.1117/12.2219319

Peer reviewed

The impact of boundary conditions and fluid velocity on damping for a fluid conveying pipe in a viscous fluid

Eric Kjolsing*[a], Michael Todd[a]
[a]Structural Engineering Department; University of San Diego, California
9500 Gilman Drive, Mail Code 0085, La Jolla, CA 92093-0085

ABSTRACT

The hydrocarbon industry has expressed interest in developing vibration based energy harvesting systems that can be deployed downhole and supplement or replace existing power sources. The energy output of such harvesters is highly dependent on the level of damping in the supporting structure which, in this case, would drive the systems vibrational input. A first step towards optimizing an energy harvester configuration is then to understand how key variables influence system damping. To this end an investigation was undertaken to identify how changing system boundary conditions effect damping in a fluid conveying pipe confined by a viscous fluid (i.e. a producing hydrocarbon well). The key variables investigated included the rotational boundary springs, the velocity of the conveyed fluid, and the viscosity of the annulus fluid. The system was modeled using Euler-Bernoulli beam theory and included a hydrodynamic forcing function to capture the effects of the viscous annulus fluid. The natural frequencies of the system were solved in the frequency domain with the system damping subsequently calculated. Lower damping ratios were observed: in stiffer systems, for lower conveyed fluid velocities, and for lower annulus fluid viscosities. A numeric example is provided to illustrate the interaction between the three variables of interest. These results are of direct interest to researchers and engineers developing vibrational energy harvesting systems for downhole deployment. Approved for publication, LA-UR-16-21227.

Keywords: Energy Harvesting, Damping, Flow-Induced Vibration, Viscous Annulus Fluid, Hydrocarbon Production, Hydrodynamic Function, Spectral Element Method, Fluid Conveying Pipe

1. INTRODUCTION

Novel vibration based energy harvesters are desired to supplement or replace existing equipment used to power downhole monitoring tools in hydrocarbon wells. The power that can be extracted using vibration based harvesters is highly dependent on the damping in the structural system to which the harvester is tuned. Under optimal harvesting conditions the harvester's natural frequency matches the predominant natural frequency of the driving accelerations (i.e. resonance) and the damping in the structural system is minimized (i.e. increased vibration amplitude). In a previous study, the authors characterized the first natural frequency of a braced hydrocarbon well.[1] In the current study, the authors seek to understand how changing the rotational boundary conditions of a braced well impacts the system damping as the conveyed fluid velocity is increased. The three independent variables investigated are the rotational stiffness of the boundary springs, the velocity of the conveyed fluid, and the viscosity of the annulus fluid (the sole source of damping in the current study). The configuration of interest is shown in Figure 1. While similar configurations have been studied by others,[2]-[9] those investigations did not sufficiently explore the relationship between the rotational boundary conditions and system damping for the current application of interest. The results of this study are intended to help researchers and engineers in the development of energy harvesting systems by characterizing the dynamics of a production string.

2. NUMERIC MODEL

Using Euler-Bernoulli theory and assuming steady plug-flow, the linearized equation of motion for a pipe conveying fluid can be written as[1],[10]

* eric.kjolsing@gmail.com

$$E^*I\dot{w}'''' + EIw'''' + \{M_iU^2 - \bar{T} + \bar{p}A_i(1-2\nu)\}w'' + 2M_iU\dot{w}' + (M_i+m)gw' + c\dot{w} + (M_i+m)\ddot{w} + i\rho_e\pi d^2\omega\Gamma U_0 e^{i\omega t} = 0, \quad (1)$$

where prime and dot indicate derivatives with respect to spatial location and time, respectively. From left to right, the forcing terms represented are: Kelvin-Voigt dissipation, flexural restoring force, centrifugal force, applied tension, pressure induced tension, Coriolis force, gravity, viscous damping, inertia, and the hydrodynamic force stemming from the annulus fluid. Positive fluid velocity (U) indicates conveyed fluid flow in the direction of gravity; noting Figure 1, fluid flow is taken as negative throughout this study.

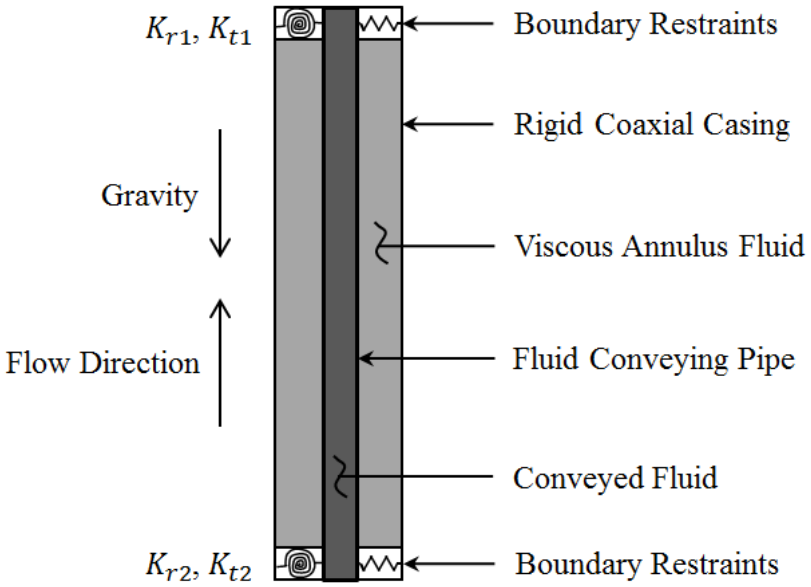

Figure 1. Modeled system.

The hydrodynamic function (Γ) is defined in Appendix B and has been thoroughly investigated by others[11]-[16]. It has been shown that the real part of the hydrodynamic function contributes added mass to the system while the imaginary part contributes viscous drag[17]. Since the hydrodynamic function is frequency dependent, changes in the rotational boundary conditions are expected to result in changes in the system damping.

Since the equation of motion is frequency dependent through the hydrodynamic forcing, the spectral element method is used to solve for the natural frequencies of the system in the frequency domain. A description of the spectral element method is available elsewhere in the literature[18],[19] and is not repeated here. Once the natural frequencies of the system are found the corresponding damping ratio can be calculated. With the translation prevented at the pipe's boundaries, the Coriolis force does no work[20],[21]. With the viscous damping (c) and Kelvin-Voigt viscosity (E^*) taken to be zero in each of the cases investigated, the only remaining damping term comes from imaginary part of the hydrodynamic function. The systems damping ratio can then be written as[15]

$$\zeta = \frac{-\rho_e\pi d^2\Gamma_i}{2(\Gamma_r\rho_e\pi d^2 + m + M_i)}. \quad (2)$$

It is important to note that in the current study the conveyed fluid flow direction at the boundaries is assumed to be tangential to the deformed pipe whose lateral translation is prevented by rigid translational springs (K_{t1} and K_{t2}). That is, the fluid momentum is assumed to be unchanging at the boundaries. This final boundary condition must be specified as research indicates that the conveyed fluid boundary conditions may influence the systems behavior for certain structural configurations[22],[23].

3. RESULTS AND DISCUSSION

Three different cases are investigated with the relevant inputs listed in Appendix C. Cases A, B, and C represent relatively low, moderate, and high viscosity annulus fluids. The inputs used are thought to be reasonable but do not necessarily coincide with any particular real-world well. Only the first mode is investigated for each case as simplifying assumptions made in the derivation of the hydrodynamic function may be violated for higher modes[24],[25].
Three dimensional damping plots can be generated for each case by specifying the rotational boundary conditions and then incrementally increasing the conveyed fluid velocity. Such a surface is illustrated in Figure 2 where case C was explored. The first rotational spring (K_{r1}) was set to 0 $\frac{Nm}{rad}$ representing a pinned boundary condition. The second rotational spring (K_{r2}) was specified as one of seven values falling between the limits of a pinned ($\frac{K_{r2}L}{EI} = 0$ $\frac{1}{rad}$) and fixed ($\frac{K_{r2}L}{EI} = 10000$ $\frac{1}{rad}$) condition. For each of the seven realizations (spanning a pinned-pinned to pinned-fixed boundary condition), the conveyed fluid velocity (U) was incrementally increased up to the bifurcation velocity (i.e. the conveyed fluid velocity at which $\zeta = 1$).

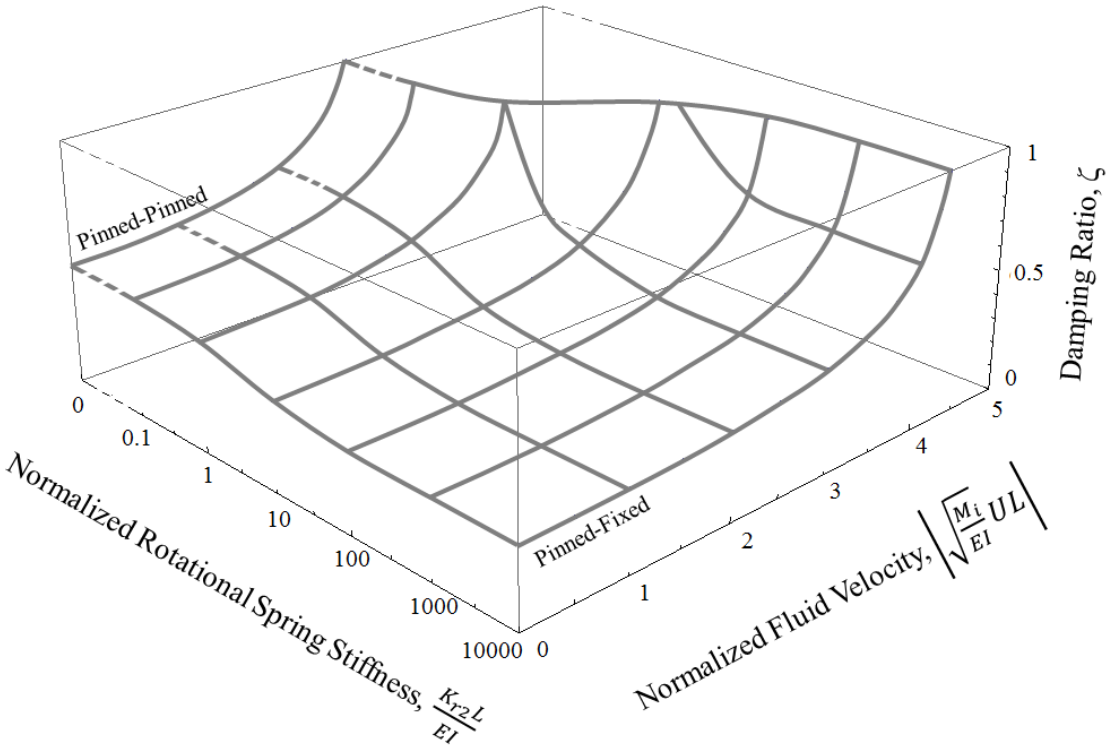

Figure 2. Damping as a function of spring stiffness and fluid velocity. Case C shown. $K_{r1} = 0$; K_{r2} = varies.

Three trends are apparent in Figure 2. First, for zero fluid flow the damping ratio is seen to increase as the boundary conditions soften (i.e. as the boundary conditions move from a pinned-fixed condition to a pinned-pinned condition). This frequency dependent behavior is explained by equation (2), which is plotted in Figure 3 for arbitrary frequency inputs. Due to the nature of the hydrodynamic function (Γ_r and Γ_i), the damping ratio is seen to increase for more flexible systems (i.e. those with smaller natural frequencies). Thus, as the system moves from a pinned-fixed to a pinned-pinned condition, the natural frequency decreases resulting in an increase in viscous drag.

The second notable trend is an increase in the damping ratio as the conveyed fluid velocity increases. This behavior is explained by the centrifugal force ($M_i U^2$) which has the effect of inducing compression in the conveying pipe. As the

fluid velocity increases, the induced compression increases, causing a decrease in the natural frequency. Again turning to Figure 3, this decrease in natural frequency results in an increase in system damping which is visible in Figure 2.

Lastly, the bifurcation velocity increases as the rotational spring stiffness is increased. This behavior is due to the boundary conditions themselves and the compression in the system induced by the centrifugal force. To simplify the explanation, consider a column under a compressive load. The column is only able to sustain a compressive load up to the Euler buckling load which is explicitly dependent on the supporting boundary conditions. Just like a pinned-fixed column is able to support a higher buckling load than a pinned-pinned column, the pinned-fixed pipe is able to support a higher compressive load (generated by the centrifugal force) than a pinned-pinned pipe.

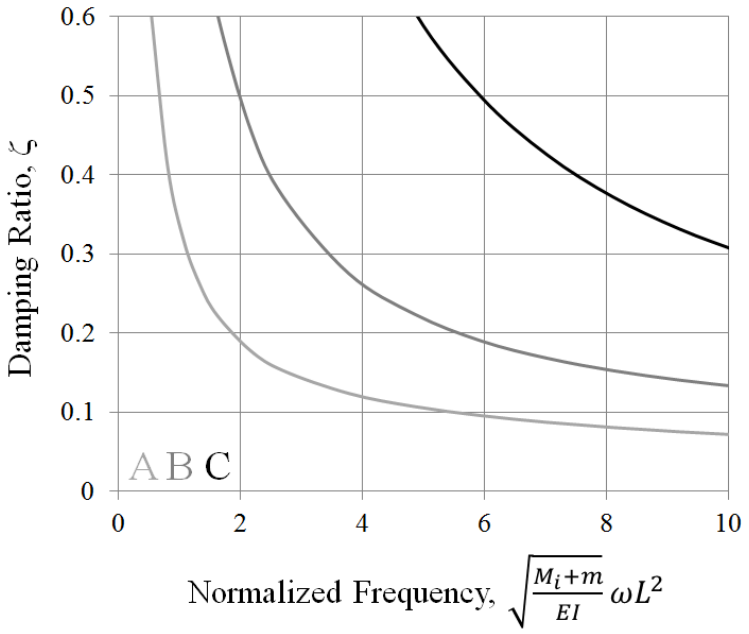

Figure 3. Frequency dependent damping ratio.

The limiting boundary conditions (P-P: pinned-pinned, P-F: pinned-fixed, F-F: fixed-fixed) can be compressed into a two-parameter plot, as shown in Figure 4. Three additional trends are noted:

1. Holding the boundary conditions and conveyed fluid velocity constant, lower viscosity systems have lower damping ratios.
2. Holding the boundary conditions constant, the bifurcation velocity increases with decreasing annulus fluid viscosity.
3. Holding the annulus fluid viscosity and conveyed fluid velocity constant, systems with more flexible rotational boundary springs have higher damping ratios.

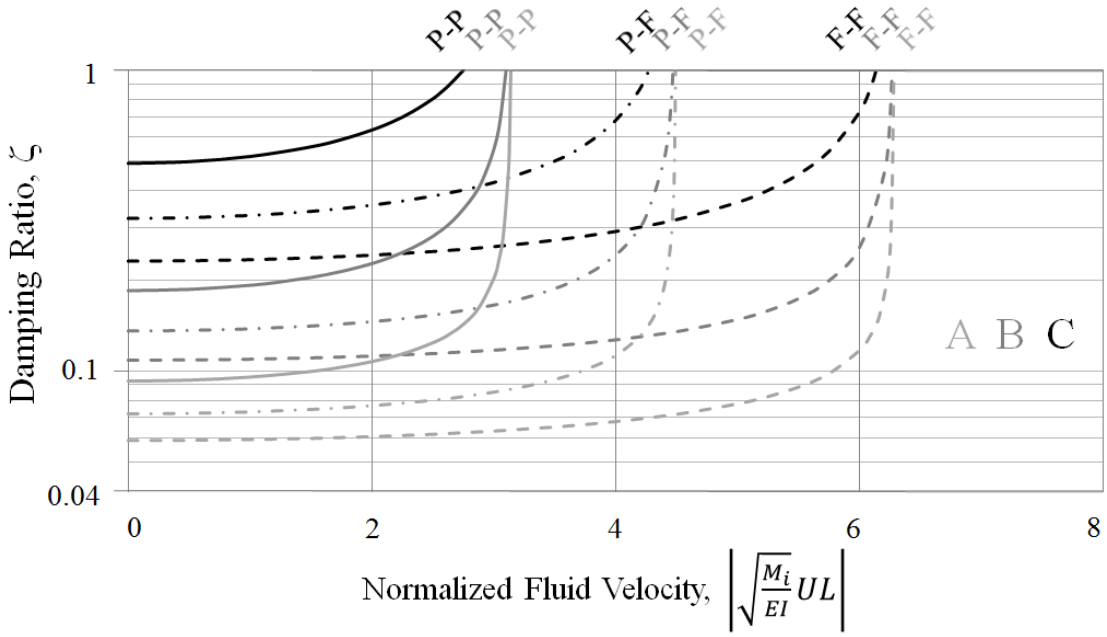

Figure 4. Damping ratio as a function of fluid velocity for three limiting boundary conditions. All three cases shown.

These results indicate that the damping ratio of a system may be underestimated should the rotational boundary conditions, produced fluid velocity, and/or annulus fluid viscosity be incorrectly estimated.

4. AN ILLUSTRATIVE EXAMPLE

Consider a design scenario in which a vibration based energy harvester is to be designed, fabricated, and deployed on a hydrocarbon production tube. For design purposes, an assumed vibration input must be developed. The harvested energy is directly related to the amplitude of the assumed vibration, which is a function of the assumed damping in the system. As has been shown, the damping in the system is directly related to the boundary conditions, produced fluid velocity, and annulus fluid viscosity. For this illustrative example, assume the damping ratio is estimated based on case A parameters (low viscosity annulus fluid), with a normalized fluid velocity of one, and rotational boundary springs with a normalized stiffness of nine. This initial realization is represented by point A_1 in Figure 5 and Figure 6. Should the actual conveyed fluid velocity be higher (A_2) or the rotational boundary springs be more flexible than expected (A_3) the actual damping in the system would be underestimated (by 11% and 26% respectively). If the annulus fluid viscosity is also underestimated (B_4), the error in the damping estimate jumps to 271%.

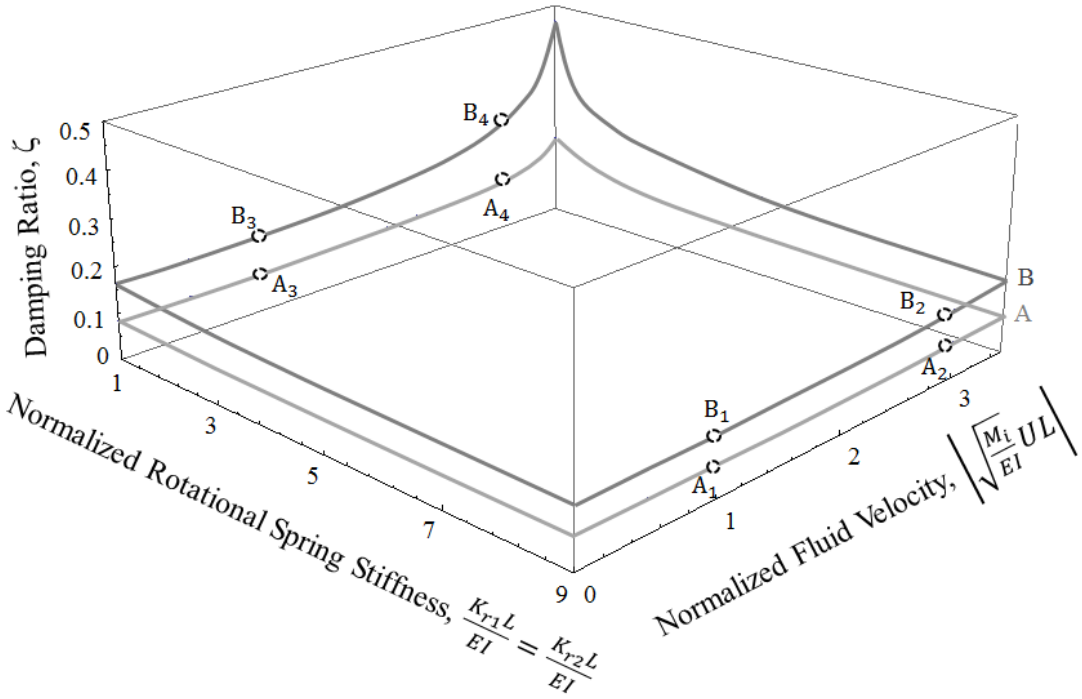

Figure 5. Potential error in damping estimates (3D).

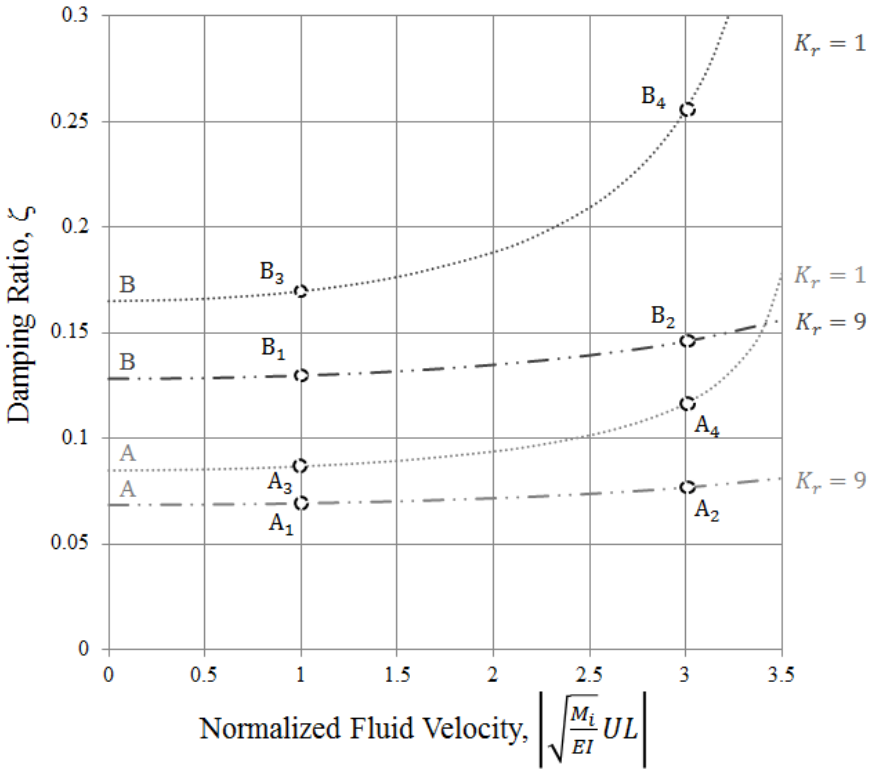

Figure 6. Potential error in damping estimates (2D).

5. SUMMARY

A novel vibration based energy harvesting system is desired for downhole deployment in producing hydrocarbon wells. Such energy harvesters are sensitive to the amplitude of vibration of the supporting structure (in this case the production tube) which is dependent on the level of damping in the system. For the current investigation, the source of damping was limited to the coaxial viscous annulus fluid which was numerically modeled by a hydrodynamic forcing function. The hydrodynamic forcing was found to be frequency dependent with higher damping ratios observed for systems operating at lower natural frequencies. Three independent variables were explored: the rotational stiffness of the boundary springs, the conveyed fluid velocity, and the annulus fluid viscosity. It was found that (1) decreasing the rotational boundary stiffness, (2) increasing the conveyed fluid velocity, and (3) increasing the annulus fluid viscosity all increased the damping ratio of the system. A numeric example was provided to illustrate the estimation errors that may result if the three independent variables investigated in this study are not properly accounted for.

ACKNOWLEDGEMENTS

Funding was provided by Los Alamos National Laboratory through the Engineering Institute under Task 5 (Subcontract No. 77137-001-11).

REFERENCES

[1] Kjolsing, E. and Todd, M., "A frequency study of a clamped-clamped pipe immersed in a viscous fluid conveying internal steady flow for use in energy harvester development as applied to hydrocarbon production wells," Proc. SPIE 9435, 943505 (2015).

[2] Kheiri, M., Païdoussis, M.P., Costa Del Pozo, G., and Amabili, M., "Dynamics of a pipe conveying fluid flexibly restrained at the ends," Journal of Fluids and Structures 49, 360-385 (2014).

[3] Bao, R., "Analysis of fluid-solid coupling characteristics of oil and gas submarine span pipelines," Journal of Pipeline Systems Engineering and Practice, A4014001 (2014).

[4] Hosseini, M., Sadeghi-Goughari, M., Atashipour, S.A., and Eftekhari, M., "Vibration analysis of single-walled carbon nanotubes conveying nanoflow embedded in a viscoelastic medium using modified nonlocal beam model," Archives of Mechanics 66(4), 217-244 (2014).

[5] Lottati, I. and Kornecki, A., "The effect of an elastic foundation and of dissipative forces on the stability of fluid-conveying pipes," Journal of Sound and Vibration 109(2), 327-338 (1986).

[6] Païdoussis, M.P., Misra, A.K., and Chan, S.P., "Dynamics and stability of coaxial cylindrical shells conveying viscous fluid," Journal of Applied Mechanics 52(2), 389-396 (1985).

[7] Païdoussis, M.P., Misra, A.K., and Nguyen, V.B., "Internal-and annular-flow-induced instabilities of a clamped-clamped or cantilevered cylindrical shell in a coaxial conduit: The effects of system parameters," Journal of Sound and Vibration 159(2), 193-205 (1992).

[8] Soltani, P., Taherian, M.M, and Farshidianfar, A., "Vibration and instability of a viscous-fluid-conveying single-walled carbon nanotube embedded in a visco-elastic medium," Journal of Physics D: Applied Physics 43(42), 425401 (2010).

[9] Yeh, T.T. and Chen, S.S., "The effect of fluid viscosity on coupled tube/fluid vibrations," Journal of Sound and Vibration 59(3), 453-467 (1978).

[10] Païdoussis, M.P. and Issid, N.T., "Dynamic stability of pipes conveying fluid," Journal of Sound and Vibration 33(3), 267-294 (1974).

[11] Stokes, G.G., [On the effect of the internal friction of fluids on the motion of pendulums, Vol. 9.], Pitt Press, (1851).

[12] Chen, S.S., "Fluid damping for circular cylindrical structures," Nuclear Engineering and Design 63(1), 81-100 (1981).

[13] Rosenhead, L., [Laminar Boundary Layers], Clarendon Press, Oxford, (1963).

[14] Tuck, E.O., "Calculation of unsteady flows due to small motions of cylinders in a viscous fluid," Journal of Engineering Mathematics 3(1), 29-44 (1969).

[15] Wambsganss, M.W., Chen, S.S., and Jendrzejczyk, J.A., "Added mass and damping of a vibrating rod in confined viscous fluids," NASA STI/Recon Technical Report N 75, 10349 (1974).

[16] Chilukuri, R., "Added mass and damping for cylinder vibrations within a confined fluid using deforming finite elements," Journal of Fluids Engineering 109(3), 283-288 (1987).
[17] Cranch, G.A., Lane, J.E., Miller, G.A., and Lou, J.W., "Low frequency driven oscillations of cantilevers in viscous fluids at very low Reynolds number," Journal of Applied Physics 113(19), 194904 (2013).
[18] Doyle, J. F., [Wave propagation in structures], Springer, US, (1989).
[19] Lee, U., [Spectral element method in structural dynamics], John Wiley & Sons, Asia, (2009).
[20] Païdoussis, M.P. and Li, G.X., "Pipes conveying fluid: a model dynamical problem," Journal of Fluids and Structures 7(2), 137-204 (1993).
[21] Païdoussis, M.P., [Fluid-structure interactions: slender structures and axial flow, Vol. 1], Academic Press, Amsterdam, (2014).
[22] Kuiper, G.L. and Metrikine, A.V., "Experimental investigation of dynamic stability of a cantilever pipe aspirating fluid," Journal of Fluids and Structures 24(4), 541-558 (2008).
[23] Païdoussis, M.P., Semler, C., and Wadham-Gagnon, M., "A reappraisal of why aspirating pipes do not flutter at infinitesimal flow," Journal of Fluids and Structures 20(1), 147-156 (2005).
[24] Basak, S., Raman, A., and Garimella, S.V., "Hydrodynamic loading of microcantilevers vibrating in viscous fluids," Journal of Applied Physics 99(11), 114906 (2006).
[25] Maali, A., Hurth, C., Boisgard, R., Jai, C., Cohen-Bouhacina, T., and Aime, J.P., "Hydrodynamics of oscillating atomic force microscopy cantilevers in viscous fluids," Journal of Applied Physics 97(7), 074907 (2005).

APPENDIX A – NOMENCLATURE

Table A.1 presents the nomenclature used throughout the manuscript

Table A.1. Nomenclature.

Dimensional Terms	
c	Viscous Damping Coefficient
d	Pipe Outer Radius
g	Coefficient of Gravity
m	Mass per Unit Length of Pipe
$\bar{p}$	Mean Pressure Differential
t	Time
w	Lateral Deflection of the Pipe
A, B, C	Investigated Cases
A_i	Flow Area
D	Confining Shell Inner Radius
E	Young's Modulus
E^*	Kelvin-Voigt Viscosity
I	Pipe Inertia
K_r	Rotational Spring Stiffness
K_t	Translational Spring Stiffness
L	Pipe Length
M_i	Mass per Unit Length of Conveyed Fluid

Dimensional Terms (cont.)	
$\bar{T}$	Externally Applied Tension
U	Mean Axial Flow Velocity
$U_0 e^{i\omega t}$	Pipe Velocity
ρ_e	Annulus Fluid Density
υ_e	Annulus Fluid Kinematic Viscosity
ω	Radial Frequency
Dimensionless Terms	
i	Imaginary Unit
I_0, I_1, K_0, K_1	Modified Bessel Functions
ζ	Equivalent Damping Ratio
ν	Poisson Ratio
Γ	Hydrodynamic Function
Γ_i	Imaginary Part of the Hydrodynamic Function
Γ_r	Real Part of the Hydrodynamic Function

APPENDIX B – HYDRODYNAMIC FUNCTION

The hydrodynamic function is written as

$$\Gamma = \frac{\Gamma_{num}}{\Gamma_{den}} - 1 = \Gamma_r - i\Gamma_i, \tag{B.1}$$

where

$$\begin{aligned}\Gamma_{num} = {} & 2\alpha^2[I_0(\alpha)K_0(\beta) - I_0(\beta)K_0(\alpha)] - 4\alpha[I_1(\alpha)K_0(\beta) + I_0(\beta)K_1(\alpha)] \\ & + 4\alpha\gamma[I_0(\alpha)K_1(\beta) + I_1(\beta)K_0(\alpha)] - 8\gamma[I_1(\alpha)K_1(\beta) - I_1(\beta)K_1(\alpha)]\end{aligned} \tag{B.2}$$

and

$$\begin{aligned}\Gamma_{den} = {} & \alpha^2(1-\gamma^2)[I_0(\alpha)K_0(\beta) - I_0(\beta)K_0(\alpha)] \\ & + 2\alpha\gamma[I_0(\alpha)K_1(\beta) - I_1(\beta)K_0(\beta) + I_1(\beta)K_0(\alpha) - I_0(\beta)K_1(\beta)] \\ & + 2\alpha\gamma^2[I_0(\beta)K_1(\alpha) - I_0(\alpha)K_1(\alpha) + I_1(\alpha)K_0(\beta) - I_1(\alpha)K_0(\alpha)].\end{aligned} \tag{B.3}$$

The relevant arguments include

$$\bar{k} = \sqrt{\frac{i\omega}{\upsilon_e}}; \quad \alpha = \bar{k}d; \quad \beta = \bar{k}D; \quad \gamma = \frac{d}{D}. \tag{B.4}$$

Assumptions used in the derivation of the hydrodynamic function include:

- The conveying pipe is an isotropic linearly elastic solid concentric to a rigid coaxial casing.
- The annulus fluid is homogeneous, Newtonian, and incompressible. Further, the annulus fluid is assumed to have zero velocity at the rigid coaxial casing and a velocity that matches the conveying pipe at the fluid-pipe interface.
- The conveying pipe is subject to small transverse displacements. Further, the pipe diameter (i.e. 2d) is much smaller than the pipe length (i.e. L).

APPENDIX C – INPUTS

The numeric inputs are shown in Table C.1.

Table C.1. Numeric inputs.

Variable	Units	Viscous Fluid Case		
		A	B	C
c	kg/s	0		
d	m	0.04		
g	m/s^2	9.81		
m	kg/m	12.52		
$\bar{p}$	N/m^2	0		
A_i	m^2	3.42E-03		
D	m	0.05		
E	N/m^2	2.00E+11		
E^*	kg/ms	0		
I	m^4	1.08E-06		
K_r	Nm/rad	Varies		
K_t	N/m	1.00E+9 (Rigid)		
L	m	8		
L^e	m	4		
M_i	kg/m	2.91		
$\bar{T}$	N	0		
U	m/s	Varies		
ρ_e	kg/m^3	850		
υ_e	m^2/s	1.00E-05	3.00E-05	9.00E-05
ν	-	0		